Geochemical Perspectives Letters

A baseline for the Sn isotopic composition of the upper continental crust

E. Kubik[1*], F. Moynier[1], J.-X. She[1,2,3], R.L. Rudnick[4]

OPEN ACCESS

https://doi.org/10.7185/geochemlet.2422

Abstract

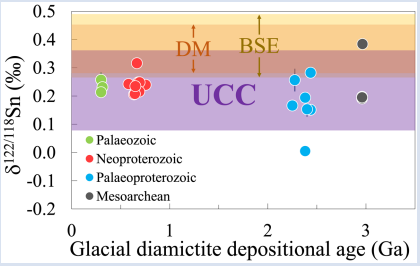

We report high precision Sn isotopic compositions, expressed as $\delta^{122/118}$Sn relative to the NIST3161a standard, for the fine grained matrix of 24 glacial diamictite composites. The diamictites were deposited from the Mesoarchean to the Palaeozoic and sampled from four continents (Africa, Asia, North and South America). They are relatively homogeneous in $\delta^{122/118}$Sn, ranging from 0.15 to 0.32 ‰ with an average $\delta^{122/118}$Sn value of 0.22 ± 0.14 ‰ (2 s.d., $n = 24$). The Sn isotopic composition of the diamictites is not influenced by chemical weathering, depositional age, geographic setting, atmospheric oxygen content or magmatic differentiation processes in the source region. As such, the average provides a robust estimate of the Sn isotopic composition of the bulk upper continental crust (UCC). This baseline is within the range of, but isotopically lighter than, the current depleted mantle estimate (0.37 ± 0.09 ‰; 2 s.d., $n = 12$) and bulk silicate Earth (0.38 ± 0.11 ‰; 2 s.d., $n = 9$). It also overlaps with the very few available measurements made on andesites, granites, a granodiorite and a rhyolite.

Received 25 December 2023 | Accepted 11 April 2024 | Published 30 May 2024

Introduction

Continents are a combined product of both differentiation and plate tectonics (Rudnick, 1995), and constitute a unique feature of Earth. As a significant planetary reservoir, the mechanisms producing continental crust, as well as the chemical and physical interactions of continents with other reservoirs, are key processes that need to be defined to understand Earth as a differentiated, dynamical planet. One clue to understanding how continental crust forms comes from its bulk major and trace element composition, which is similar to that of magmas found above subduction zones (*e.g.*, Rudnick, 1995; Tatsumi, 2008). However, the continental crust is highly heterogeneous, posing a significant challenge in estimating its average composition. Nevertheless, making such estimates is necessary to understand its origin and its contribution to element cycles within the bulk silicate Earth. Because of intracrustal differentiation, incompatible elements are concentrated in the upper continental crust (UCC), making this region the most critical for understanding the bulk crust composition. Estimates of the average composition of the UCC have primarily been obtained through two approaches: large scale bedrock sampling with grid-based averages and analyses of fine grained sedimentary rocks such as shales, loess and the matrix of glacial diamictites (*e.g.*, Rudnick and Gao, 2014; Gaschnig *et al.*, 2016).

Here we use the fine grained matrix of glacial diamictites to estimate the stable isotope composition of tin (Sn) in the UCC and use these results to infer crustal formation and evolution processes. We compare this result with that of igneous rocks. This UCC estimate can be used as a baseline for studying Sn mineralisation, with implications for ore-forming processes (Zhou *et al.*, 2022; Wu *et al.*, 2023).

Tin is a moderately siderophile, chalcophile and volatile element (Jochum *et al.*, 1993). It exhibits incompatible and lithophile behaviour during igneous differentiation and, as such, is concentrated in the crust relative to the mantle. In magmatic systems, Sn is incompatible in most phases but compatible in ilmenite, its main host, where it exists as VI fold coordinated Sn^{4+} (Klemme *et al.*, 2006; Rudnick and Gao, 2014). Within the continental crust, Sn is concentrated in highly evolved granitic magmas derived from partial melting of metapelitic rocks (Jochum *et al.*, 1993). Systematic element distribution patterns in these granites point to fractional crystallisation as the main process controlling magmatic evolution and Sn enrichment (Lehmann, 2021). All Sn — a medium scale "critical metal" — production originates from continental crustal ore deposits consisting of Sn granites, pegmatites and Sn porphyries (Lehmann, 2021). Finally, Sn is an insoluble element that is not mobilised during chemical weathering (White, 2018).

Tin is concentrated in dense minerals of the continental crust, which are likely sorted during wind- or water-driven transport (Gaschnig *et al.*, 2016), which hinders using the geochemistry of wind- or water-transported sedimentary rocks (*e.g.*, shales, periglacial and desert loess) to obtain a robust Sn

1. Université Paris Cité, Institut de Physique du Globe de Paris, CNRS, UMR 7154, 1 rue Jussieu, 75005 Paris, France
2. State Key Laboratory for Mineral Deposits Research, School of Earth Sciences and Engineering, Nanjing University, Nanjing, Jiangsu 210023, China
3. Frontiers Science Center for Critical Earth Material Cycling, Nanjing University, Nanjing, China
4. Department of Earth Science and Earth Research Institute, University of California, Santa Barbara, CA 93105, United States
* Corresponding author: (email: edith.kubik@gmail.com)

isotopic composition for the UCC. On the other hand, glacial diamictites, which are produced by mechanical erosion of the bedrock by glaciers, deposited in the form of glacial till, and subsequently lithified in a rapid and low temperature process that minimises chemical weathering (Li *et al.*, 2016), may be a useful means to estimate the Sn isotopic composition of the UCC. Tin is one of the few trace elements that shows secular increase in abundance in glacial deposits through time (Gaschnig *et al.*, 2016) due to its incompatible behaviour. Significant Sn isotope fractionation has been reported in terrestrial samples (Badullovich *et al.*, 2017; Wang *et al.*, 2018) and in a number of geological processes such as liquid-vapour separation (She *et al.*, 2020), redox processes (Roskosz *et al.*, 2020), metal–silicate equilibrium (Kubik *et al.*, 2021), and hydrothermal processes (Liu *et al.*, 2021), indicating that Sn isotopes may be fractionated during continental crust formation. This raises the question of whether there may also be a secular evolution of the Sn isotopic composition in glacial diamictites. In this study, we use glacial diamictite composites derived from units with depositional ages spanning 3 Ga and collected from four continents to study secular changes, geographic influence, the effects of chemical weathering and magmatic differentiation on $\delta^{122/118}$Sn and to calculate an average Sn isotopic composition of the UCC.

Materials and Methods

Glacial diamictites are produced by mechanical erosion of Earth's surface by ice sheets, which dump their load upon melting. Many, though not all of the 24 diamictite composites investigated here were deposited in a shallow marine environment and are, by definition, unsorted and experienced little post-depositional weathering (Li *et al.*, 2016). Many are unmetamorphosed, but some experienced up to greenschist facies conditions (Gaschnig *et al.*, 2016; Han *et al.*, 2023). The diamictites have depositional ages between 2.9 and 0.3 Ga, and wide geographic origins, spanning four modern continents. These samples were previously analysed for their major and trace element compositions (Gaschnig *et al.*, 2014, 2016), for their stable Li, N, O, Si, K, Ti, V, Fe, Ni, Zr, Mo, Ba, Ce isotopes, radiogenic Sm-Nd, Hf-W, Re-Os isotope compositions (full listing of these studies in Li *et al.*, 2023), and U-Pb and Lu-Hf analyses of detrital zircon (Gaschnig *et al.*, 2022). These studies demonstrated that, although there is great chemical heterogeneity in the individual samples and even in the composites, the samples nevertheless can be used to estimate the average composition of the UCC (*e.g.*, Gaschnig *et al.*, 2016).

Tin purification and subsequent isotope measurements were performed in a class-100 clean room environment using class-10 laminar flow hoods at the Institut de Physique du Globe de Paris. Tin purification uses the ion exchange chromatography and measurements employ a double spike protocol described in Creech *et al.* (2017). Tin isotope ratios were measured using a Thermo-Scientific Neptune Plus. The purification method and analytical parameters are detailed in the Supplementary Information.

Results

All Sn isotopic ratios herein are expressed as $\delta^{122/118}$Sn relative to the NIST3161a standard and uncertainties are 2 standard deviations. The glacial diamictites are generally isotopically homogeneous, except for two outliers (0.00 and 0.38 ‰), with $\delta^{122/118}$Sn values between 0.15 and 0.32 ‰ with an average of 0.22 ± 0.14 ‰. These values overlap with the very few measurements performed on granite and granodiorite reference materials (from 0.20 to 0.52 ‰; Creech *et al.*, 2017; Wang *et al.*, 2022; She *et al.*, 2023b), and are isotopically heavier than peridotites (average of −0.03 ± 0.49 ‰; Wang *et al.*, 2018).

Discussion

Tin shows a secular increase in abundance with time in the diamictite composites (Gaschnig *et al.*, 2016), with higher concentrations in the Neoproterozoic and Palaeozoic than Mesoarchean and Palaeoproterozoic samples. This is attributed to its incompatible behaviour and therefore preferential partitioning into melt during partial melting and crystal fractionation. Despite this increase in concentration, there is no resolvable change in the $\delta^{122/118}$Sn values of glacial diamictites through time (Fig. 1a). This is in agreement with the Sn isotopic ratios measured in komatiites (Badullovich *et al.*, 2017), which show that samples across a wide range of degrees of partial melting produce variable Sn abundances in the melts, but identical Sn isotopic compositions. Thus, the transition from mafic to felsic UCC at the end of the Archean does not translate into a change of Sn isotopic composition. This absence of secular change therefore suggests a relatively constant Sn isotopic composition of the

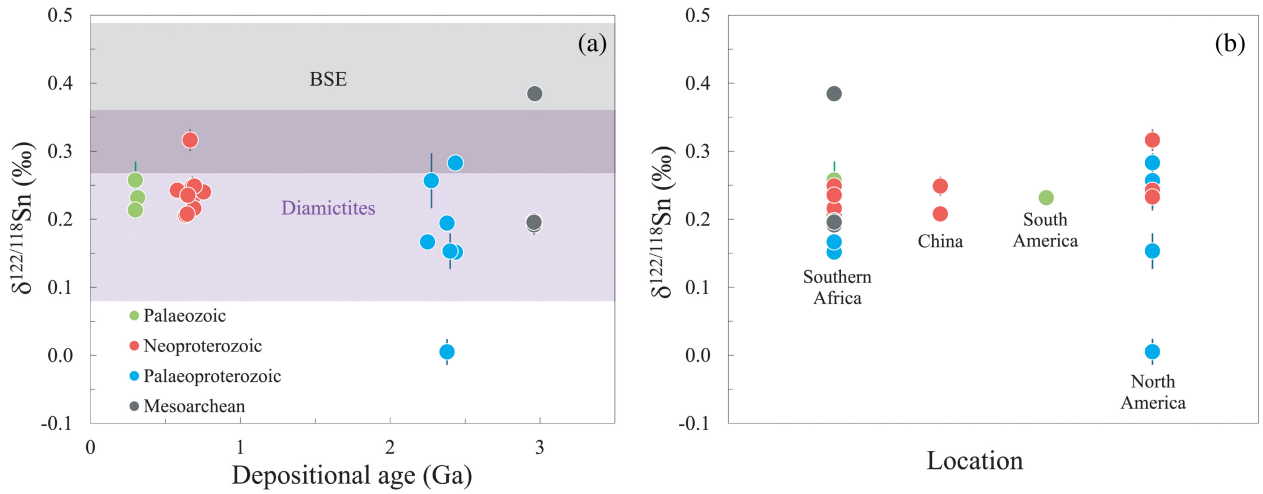

Figure 1 **(a)** $\delta^{122/118}$Sn as a function of the depositional age of the glacial diamictites. **(b)** $\delta^{122/118}$Sn of the measured glacial diamictites sorted by locations. Here and in subsequent figures, the symbols are colour coded according to the depositional age.

UCC since the Mesoarchean. Moreover, there is no clear correlation between the Sn isotopic compositions of glacial diamictites and their geographic location (Fig. 1b), demonstrating a widespread spatial homogeneity of the UCC with respect to Sn isotopic compositions.

The diamictites record variable weathering signatures, which mostly reflect the material that the glaciers sampled (Li *et al.*, 2016). We therefore evaluated potential chemical weathering effects on Sn isotopes. Chemical weathering proxies include the chemical index of alteration (CIA, corresponding to molar $Al_2O_3/(Al_2O_3 + K_2O + Na_2O + CaO^*)$ with CaO* corrected to remove the contribution of apatite and carbonate) and Al_2O_3/SiO_2 which increases due to Al_2O_3 enrichment during clay formation (Gaschnig *et al.*, 2014). The Sn isotopic compositions of glacial diamictites reported in this study do not correlate with any of these proxies (Fig. 2), consistent with Sn's low solubility (White, 2018) and indicating that chemical weathering did not fractionate Sn isotopes. Therefore, glacial diamictites can be used to (1) establish an average Sn isotopic composition of the UCC, and (2) study other processes influencing UCC composition, such as igneous differentiation, without these signatures being obscured by chemical weathering effects.

The effect of the transition from mafic to more felsic crustal sources on the Sn isotopic composition of glacial diamictites was assessed using two different proxies for igneous differentiation (Fig. 3). The Th/Sc ratio can be used to distinguish mafic from felsic sources due to the compatible behaviour of Sc as opposed to the incompatible behaviour of Th, with high Th/Sc therefore indicating a granitic source. The Th/Sc of the diamictite composites increases between the Mesoarchean and Palaeoproterozoic and remains constant thereafter (Gaschnig *et al.*, 2016) while the Ni/Lu ratio decreases exponentially from the Mesoarchean, which sampled a UCC with very high Ni abundance. There is no correlation between either of these proxies and the Sn isotopic compositions in the glacial diamictites. This indicates that Sn isotopes are largely unaffected by crustal differentiation over time and by the possible evolution of the crustal source from mafic to a more felsic composition.

Two diamictite composites, Mozaan (0.38 ± 0.01 ‰) and Bruce (0.00 ± 0.02 ‰) are significant outliers in terms of their Sn isotopic signatures, though their Sn abundances are not anomalous. The Archean Mozaan diamictite contains exceptionally high Fe_2O_3, high magnetite content (Han *et al.*, 2023), low SiO_2 and Al_2O_3 abundances, and very low $\delta^{30}Si$ (Murphy *et al.*, 2022), interpreted as reflecting a significant contribution from banded Fe formation (Gaschnig *et al.*, 2014; Murphy *et al.*, 2022). This suggests that magnetite that precipitates from seawater may preferentially incorporate the heavy isotopes of Sn. The origin of the light Sn isotopic signature measured in the Bruce diamictite remains unclear but could be attributed to a change in redox conditions, which can translate into Sn isotopic fractionation.

The Sn isotopic composition of glacial diamictite composites is not significantly influenced by chemical weathering, depositional age, geographic setting, or average UCC compositional changes due to igneous differentiation processes. The $\delta^{122/118}Sn$ of these samples thus provide an ideal means by which to derive a robust estimate of the Sn isotopic composition of the UCC. The arithmetic mean of $\delta^{122/118}Sn$ in all measured diamictites corresponds to 0.22 ± 0.14 ‰ (2 s.d., $n = 24$). This UCC Sn isotopic estimate is on the lower side but within error of the depleted mantle (0.37 ± 0.09 ‰, as sampled by mid-ocean ridge basalts; She *et al.*, 2023a), and two BSE estimates based on komatiites (0.38 ± 0.11 ‰) and a peridotite (0.17 ± 0.07 ‰) (Fig. 4).

Significant Sn isotope fractionation has been reported to occur through three igneous processes: ilmenite-melt fractionation (Badullovich *et al.*, 2017), redox changes (Roskosz *et al.*, 2020) and during partial melting (Wang *et al.*, 2018). Here, we evaluate the potential of each of these processes in establishing the Sn isotopic composition of the UCC.

Ilmenite crystallisation has been proposed as a fractionating process during magmatic differentiation, based on a suite of samples from the Kilauea Iki lava lake (Badullovich *et al.*, 2017). Ilmenite crystallisation is predicted to enrich silicate melts in light Sn isotopes, which could explain the observed offset between the Sn isotopic compositions of the diamictites and that of MORB and komatiites (Fig. 4). We also note identical Sn isotopic signatures measured in the basalt-andesite and andesite samples of the Kilauea suite and in the glacial diamictites. However, this process is more likely to generate intracrustal heterogeneities as opposed to fractionating Sn isotopes in the continental crust with respect to the mantle, thus shifting the bulk isotopic composition of the UCC. Indeed, in Badullovich *et al.* (2017), the differentiation suite from basalt to andesite generates a 0.20 ‰ difference between the end members which correlates with TiO_2. However, the evolution of the continental crust from mafic to felsic does not produce such a trend in Sn isotopic ratios (Fig. 1a) and Sn isotopes do not correlate with TiO_2 (Fig. 3d).

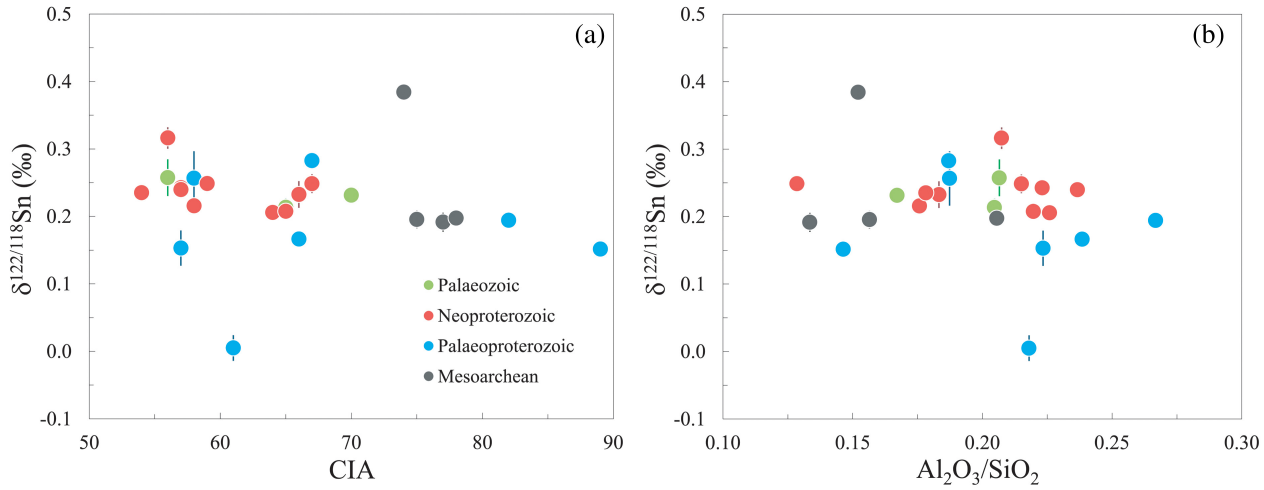

Figure 2 $\delta^{122/118}Sn$ of glacial diamictites as a function of two indicators of chemical weathering: **(a)** CIA (chemical index of alteration) values and **(b)** Al_2O_3/SiO_2. All elemental compositions used are from Gaschnig *et al.* (2016).

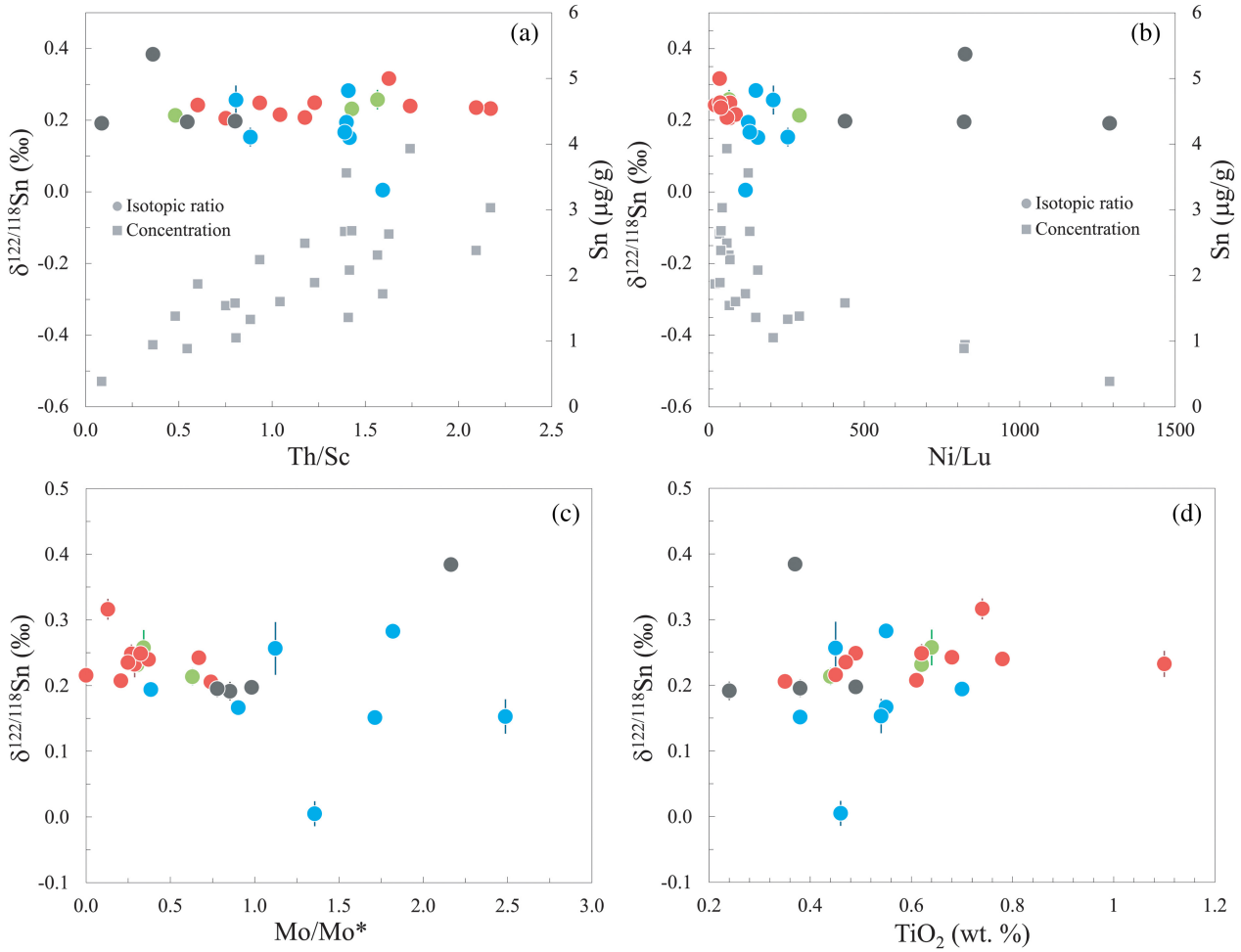

Figure 3 $\delta^{122/118}$Sn of glacial diamictites as a function of two differentiation indicators: **(a)** Th/Sc ratio, including Sn abundances in the corresponding samples, and **(b)** Ni/Lu ratio, as well as **(c)** Mo/Mo*, a proxy for oxidative weathering (Gaschnig *et al.*, 2014) and **(d)** TiO_2 abundance, an indicator of ilmenite crystallisation. All trace element data were compiled from Gaschnig *et al.* (2016).

In fact, the Sn isotopic variability within our data set, excluding outliers, is <0.20 ‰ as the diamictites range from 0.15 to 0.32 ‰, suggesting that ilmenite crystallisation did not play a major role in fractionating the Sn isotopic composition of the continental crust from the mantle.

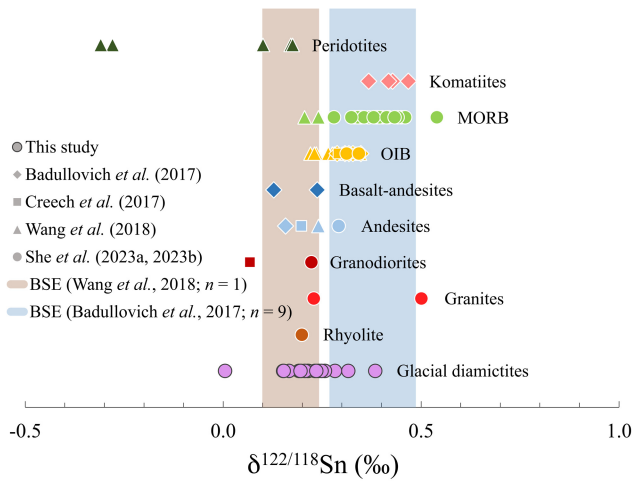

Figure 4 Tin isotopic compositions expressed as $\delta^{122/118}$Sn of terrestrial igneous samples (Badullovich *et al.*, 2017; Creech *et al.*, 2017; Wang *et al.*, 2018; She *et al.*, 2023a, 2023b) compared to those of glacial diamictite composites analysed in this study.

First principle calculations (Wang *et al.*, 2021) and nuclear resonant inelastic X-ray scattering studies (Polyakov *et al.*, 2005; Roskosz *et al.*, 2020) have also shown that the force constants of Sn substantially increase from Sn^{2+}- to Sn^{4+}-bearing materials, implying that heavy Sn isotopes are enriched in Sn^{4+}- relative to Sn^{2+}-bearing materials. As Sn^{4+} is more incompatible than Sn^{2+}, the continental crust ought to be enriched in heavy Sn isotopes compared to MORB. However, the UCC Sn isotopic estimate derived from our measurements is within error of MORB samples (Fig. 4) and depleted mantle estimates (She *et al.*, 2023a). This suggests that the isotopic fractionation identified from different Sn force constants measured between Sn^{4+}- and Sn^{2+}-bearing synthesised melts (Roskosz *et al.*, 2020) is not the main process establishing the Sn isotopic composition of the UCC. Additionally, we tested the influence of oxidative weathering on the Sn isotopic composition of the diamictites (Gaschnig *et al.*, 2014). There is no correlation between our data and Mo/Mo* (Fig. 3c) demonstrating that the Sn isotopic composition of the diamictites is not affected by secondary redox related processes.

The fractionation of Sn isotopes during partial melting has been proposed based on the observed offset between the isotopic composition of basalts and peridotites (Wang *et al.*, 2018). However, the melt products appear to be unaffected by

the percentage of partial melting, as the Sn isotopic compositions across a series of komatiites reflecting a wide range of degrees of melting (Badullovich *et al.*, 2017), and MORB from ridges with very different spreading rates (She *et al.*, 2023a) are similar. The currently limited data available for Sn isotopic ratios in peridotites shows a large variability that hampers deciphering magmatic processes. Moreover, our Sn isotope UCC estimate based on glacial diamictite analysis — which is constant through time and uncorrelated to any proxy — suggests that the continental crust was formed from a source that had a constant bulk Sn isotopic composition, not significantly different from that of the UCC. The BSE is therefore likely to have a similar signature to the depleted mantle, in agreement with the identical estimates of the depleted MORB mantle (0.37 ± 0.09 ‰; She *et al.*, 2023a) and BSE of Badullovich *et al.* (2017) corresponding to 0.38 ± 0.11 ‰. Both these estimates largely overlap within error with the proposed UCC estimate derived from our measurements. Measurements of Zr isotopes in the glacial diamictites also yield compositions that are constant through time but slightly heavier than the BSE, which has been interpreted as a large scale mixing of isotopically heavy felsic material with isotopically light mantle-like mafic material (Tian *et al.*, 2021). In the case of Sn, available data for felsic igneous rocks (Fig. 4) are not particularly isotopically light, suggesting that such a mixing process is not required to explain the slightly isotopically light signature of the UCC. However, very few data are available for evolved igneous rocks and future studies on this topic are expected to bring new insight regarding Sn isotope behaviour in igneous rocks.

Synthesis

We propose a new estimate for the Sn isotopic composition of the UCC based on high precision measurements of glacial diamictite composites of 0.22 ± 0.14 ‰ (2 s.d., $n = 24$). The Sn isotopic composition of the diamictites is not influenced by chemical weathering, depositional age, geographic setting, igneous differentiation or any of the previously reported Sn-fractionating processes. Our data suggest limited fractionation between the BSE, the depleted MORB mantle and the UCC, in agreement with previous studies investigating Sn isotope behaviour in magmatic processes (Badullovich *et al.*, 2017; Creech *et al.*, 2017; She *et al.*, 2023a, 2023b). Moreover, our estimate for the UCC Sn isotopic composition provides a useful baseline to study isotope fractionation during cassiterite crystallisation (Wu *et al.*, 2023) with direct applications for tracing Sn mineralisations (Zhou *et al.*, 2022).

Acknowledgements

The authors thank two anonymous reviewers and editor Raúl Fonseca for their detailed reviews which greatly improved our manuscript. We thank Pascale Louvat and Dimitri Rigoussen for their technical support during MC-ICP-MS measurements. FM acknowledges funding from the ERC METAL (No. 101001282) and the UnivEarthS Labex program (ANR-10-LABX-0023 and ANR-11-IDEX-0005-02). This research work was supported by the IPGP analytical platform PARI, region Île-de-France SESAME Grant No. 12015908 and DIM ACAV+.

Editor: Raul O.C. Fonseca

Additional Information

Supplementary Information accompanies this letter at https://www.geochemicalperspectivesletters.org/article2422.

Cite this letter as: Kubik, E., Moynier, F., She, J.-X., Rudnick, R.L. (2024) A baseline for the Sn isotopic composition of the upper continental crust. *Geochem. Persp. Let.* 30, 51–56. https://doi.org/10.7185/geochemlet.2422

References

Badullovich, N., Moynier, F., Creech, J., Teng, F.-Z., Sossi, P.A. (2017) Tin isotopic fractionation during igneous differentiation and Earth's mantle composition. *Geochemical Perspectives Letters* 5, 24–28. https://doi.org/10.7185/geochemlet.1741

Creech, J.B., Moynier, F., Badullovich, N. (2017) Tin stable isotope analysis of geological materials by double-spike MC-ICPMS. *Chemical Geology* 457, 61–67. https://doi.org/10.1016/j.chemgeo.2017.03.013

Gaschnig, R.M., Rudnick, R.L., McDonough, W.F., Kaufman, A.J., Hu, Z., Gao, S. (2014) Onset of oxidative weathering of continents recorded in the geochemistry of ancient glacial diamictites. *Earth and Planetary Science Letters* 408, 87–99. https://doi.org/10.1016/j.epsl.2014.10.002

Gaschnig, R.M., Rudnick, R.L., McDonough, W.F., Kaufman, A.J., Valley, J.W., Hu, Z., Gao, S., Beck, M.L. (2016) Compositional evolution of the upper continental crust through time, as constrained by ancient glacial diamictites. *Geochimica et Cosmochimica Acta* 186, 316–343. https://doi.org/10.1016/j.gca.2016.03.020

Gaschnig, R.M., Horan, M.F., Rudnick, R.L., Vervoort, J.D., Fisher, C.M. (2022) History of crustal growth in Africa and the Americas from detrital zircon and Nd isotopes in glacial diamictites. *Precambrian Research* 373, 106641. https://doi.org/10.1016/j.precamres.2022.106641

Han, P.-Y., Rudnick, R.L., He, T., Marks, M.A.W., Wang, S.-J., Gaschnig, R.M., Hu, Z.-C. (2023) Halogen (F, Cl, Br, and I) concentrations of the upper continental crust through time as recorded in ancient glacial diamictite composites. *Geochimica et Cosmochimica Acta* 341, 28–45. https://doi.org/10.1016/j.gca.2022.11.012

Jochum, K.P., Hofmann, A.W., Seufert, H.M. (1993) Tin in mantle-derived rocks: Constraints on Earth evolution. *Geochimica et Cosmochimica Acta* 57, 3585–3595. https://doi.org/10.1016/0016-7037(93)90141-I

Klemme, S., Günther, D., Hametner, K., Prowatke, S., Zack, T. (2006) The partitioning of trace elements between ilmenite, ulvospinel, armalcolite and silicate melts with implications for the early differentiation of the moon. *Chemical Geology* 234, 251–263. https://doi.org/10.1016/j.chemgeo.2006.05.005

Kubik, E., Siebert, J., Mahan, B., Creech, J., Blanchard, I., Agranier, A., Shcheka, S., Moynier, F. (2021) Tracing Earth's Volatile Delivery With Tin. *Journal of Geophysical Research: Solid Earth* 126, e2021JB022026. https://doi.org/10.1029/2021JB022026

Lehmann, B. (2021) Formation of tin ore deposits: A reassessment. *Lithos* 402–403, 105756. https://doi.org/10.1016/j.lithos.2020.105756

Li, S., Gaschnig, R.M., Rudnick, R.L. (2016) Insights into chemical weathering of the upper continental crust from the geochemistry of ancient glacial diamictites. *Geochimica et Cosmochimica Acta* 176, 96–117. https://doi.org/10.1016/j.gca.2015.12.012

Li, W., Nakada, R., Takahashi, Y., Gaschnig, R.M., Hu, Y., Shakouri, M., Rudnick, R.L., Liu, X.-M. (2023) Cerium geochemical composition of the upper continental crust through time: Implications for tracing past surface redox conditions. *Geochimica et Cosmochimica Acta* 359, 20–29. https://doi.org/10.1016/j.gca.2023.08.024

Liu, P., Mao, J., Lehmann, B., Weyer, S., Horn, I., Mathur, R., Wang, F., Zhou, Z. (2021) Tin isotopes via fs-LA-MC-ICP-MS analysis record complex fluid

evolution in single cassiterite crystals. *American Mineralogist* 106, 1980–1986. https://doi.org/10.2138/am-2021-7558

Murphy, M.E., Savage, P.S., Gardiner, N.J., Prave, A.R., Gaschnig, R.M., Rudnick, R.L. (2022) Homogenising the upper continental crust: The Si isotope evolution of the crust recorded by ancient glacial diamictites. *Earth and Planetary Science Letters* 591, 117620. https://doi.org/10.1016/j.epsl.2022.117620

Polyakov, V.B., Mineev, S.D., Clayton, R.N., Hu, G., Mineev, K.S. (2005) Determination of tin equilibrium isotope fractionation factors from synchrotron radiation experiments. *Geochimica et Cosmochimica Acta* 69, 5531–5536. https://doi.org/10.1016/j.gca.2005.07.010

Roskosz, M., Amet, Q., Fitoussi, C., Dauphas, N., Bourdon, B., Tissandier, L., Hu, M.Y., Said, A., Alatas, A., Alp, E.E. (2020) Redox and structural controls on tin isotopic fractionations among magmas. *Geochimica et Cosmochimica Acta* 268, 42–55. https://doi.org/10.1016/j.gca.2019.09.036

Rudnick, R.L. (1995) Making continental crust. *Nature* 378, 571–578. https://doi.org/10.1038/378571a0

Rudnick, R.L., Gao, S. (2014) 4.1 - Composition of the Continental Crust. In: Holland, H.D., Turekian, K.K. (Eds.) *Treatise on Geochemistry*. Second Edition, Elsevier, Hoboken, 1–51. https://doi.org/10.1016/B978-0-08-095975-7.00301-6

She, J.-X., Wang, T., Liang, H., Muhtar, M.N., Li, W., Liu, X. (2020) Sn isotope fractionation during volatilization of Sn(IV) chloride: Laboratory experiments and quantum mechanical calculations. *Geochimica et Cosmochimica Acta* 269, 184–202. https://doi.org/10.1016/j.gca.2019.10.033

She, J.-X., Kubik, E., Li, W., Moynier, F. (2023a) Stable Sn isotope signatures of Mid-ocean ridge basalts. *Chemical Geology* 622, 121347. https://doi.org/10.1016/j.chemgeo.2023.121347

She, J.-X., Li, W., An, S., Cai, Y. (2023b) High-precision double-spike Sn isotope analysis of geological materials by MC-ICP-MS. *Journal of Analytical Atomic Spectrometry* 38, 142–155. https://doi.org/10.1039/D2JA00339B

Tatsumi, Y. (2008) Making continental crust: The sanukitoid connection. *Chinese Science Bulletin* 53, 1620–1633. https://doi.org/10.1007/s11434-008-0185-9

Tian, S., Moynier, F., Inglis, E.C., Rudnick, R.L., Huang, F., Chauvel, C., Creech, J.B., Gaschnig, R.M., Wang, Z., Guo, J.-L. (2021) Zirconium isotopic composition of the upper continental crust through time. *Earth and Planetary Science Letters* 572, 117086. https://doi.org/10.1016/j.epsl.2021.117086

Wang, T., She, J.-X., Yin, K., Wang, K., Zhang, Y., Lu, X., Liu, X., Li, W. (2021) Sn(II) chloride speciation and equilibrium Sn isotope fractionation under hydrothermal conditions: A first principles study. *Geochimica et Cosmochimica Acta* 300, 25–43. https://doi.org/10.1016/j.gca.2021.02.023

Wang, X., Amet, Q., Fitoussi, C., Bourdon, B. (2018) Tin isotope fractionation during magmatic processes and the isotope composition of the bulk silicate Earth. *Geochimica et Cosmochimica Acta* 228, 320–335. https://doi.org/10.1016/j.gca.2018.02.014

Wang, Z.-Y., Luo, Z.-Y., Zhang, L., Liu, J.-J., Li, J. (2022) Sn Isotopic Values in Ten Geological Reference Materials by Double-Spike MC-ICP-MS. *Geostandards and Geoanalytical Research* 46, 547–561. https://doi.org/10.1111/ggr.12443

White, W.M. (2018) Tin. In: White, W.M. (Ed.) *Encyclopedia of Geochemistry*. Springer, Cham, 1443–1445. https://doi.org/10.1007/978-3-319-39312-4_297

Wu, J., Li, H., Mathur, R., Bouvier, A., Powell, W., Yonezu, K., Zhu, D. (2023) Compositional variation and Sn isotope fractionation of cassiterite during magmatic-hydrothermal processes. *Earth and Planetary Science Letters* 613, 118186. https://doi.org/10.1016/j.epsl.2023.118186

Zhou, Z.-H., Mao, J.-W., Zhao, J.-Q., Gao, X., Weyer, S., Horn, I., Holtz, F., Sossi, P.A., Wang, D.-C. (2022) Tin isotopes as geochemical tracers of ore-forming processes with Sn mineralization. *American Mineralogist* 107, 2111–2127. https://doi.org/10.2138/am-2022-8200

Geochemical Perspectives Letters

A baseline for the Sn isotopic composition of the upper continental crust

E. Kubik, F. Moynier, J.-X. She, R.L. Rudnick

Supplementary Information

The Supplementary Information includes:

- Analytical Method
- Geological Reference Material Analysis
- Tables S-1 and S-2
- Supplementary Information References

Analytical Method

Glacial diamictite powders obtained as described in Gaschnig *et al.* (2016) were carefully weighed. To pre-cleaned Teflon beakers, ca. 500 mg of powdered sample were double-spiked (using Sn abundance estimates from Gaschnig *et al*., 2016) and added 5 mL of concentrated nitric acid and 5 mL of concentrated HF, and left on a hotplate at 100ºC for 48 hours to digest. They were dried down and taken up in aqua regia at 150 °C for 24 hours to dissolve fluoride complexes. The samples were evaporated and added 5 mL of 10 N HCl and re-evaporated to dryness before finally making them into 2 mL of 0.5 N HCl solutions adequate for the anion-exchange chemistry protocol. The samples were loaded on 1 mL of Eichrom TRU resin contained in Biorad columns and conditioned with 4 mL of 0.5 N HCl. The matrix was eluted in 4 mL of 0.5 N HCl, 4 + 3 mL of 0.25 N HCl, and the Sn cuts were collected in 4 + 3 + 3 mL of 0.5 N HNO_3. One mL of 10 N HCl was added to the clean beakers prior to Sn collection to avoid the formation of insoluble compounds in the Sn-HNO_3 mixture.

Sample Sn stable isotope ratios were measured using a Thermo-Scientific Neptune Plus multi-collector inductively coupled plasma mass spectrometer operating in low-resolution mode. The sample solutions were introduced using an ESI Apex desolvation system and a PFA nebuliser with an uptake rate of 100 µL min^{-1}. In between sample measurements, three rinse cycles were performed using three different clean 0.5 N HCl solutions after which the on-peak zero was measured. Groups of two samples were bracketed by measurements of optimally double-spiked standards. The data reduction was carried out using Isospike (www.isospike.org; Creech and Paul, 2015; Creech *et al*., 2017) operated with the Iolite software. Tin isotopic ratios are reported with delta notation as $\delta^{122/118}$Sn relative to the NIST3161a standard and 2 standard deviations. Procedural blanks were measured and found insignificant compared to the Sn abundance in the measured samples (<1 ng). The external reproducibility of the protocol was ensured by processing two geological reference materials: BHVO-2 and BCR-2. The internal reproducibility of the method was tested by performing full replicates (double-spiking, dissolution and chemical separation): two replicates of BHVO-2 and four replicates of BCR-2.

Geological Reference Material Analysis

The $\delta^{122/118}$Sn value determined for BHVO-2 is 0.36 ± 0.01 ‰ and shows excellent reproducibility between the two replicates (0.37 ± 0.04 ‰ and 0.35 ± 0.06 ‰, with n = 4 and 3, respectively) and with literature data (0.33 ± 0.01 ‰; She *et al.*, 2023). Similar results are inferred from BCR-2 measurements which yield an average of 0.28 ± 0.01 ‰ over four full replicates and a total of 11 individual measurements. The yields of the purification process were estimated using the exact digested masses and the Sn concentration estimates from Gaschnig *et al*. (2016) and have typical values and dispersion for Sn purification (Creech *et al*., 2017): from 6.6 to 48.8 % with an average of 25.3 %. Although these values are arguably low, the four full replicates of BCR-2 with different yields (7.6, 29.5, 45.6 and 48.4 %) produced identical isotopic composition values within error (0.29 ± 0.01 ‰, 0.27 ± 0.04 ‰, 0.29 ± 0.03 ‰ and 0.27 ± 0.02 ‰ respectively), suggesting that the yield does not influence the accuracy of the isotopic measurements. The same is observed with both BHVO-2 full replicates (yields of 20.7 % and 40.3 % and $\delta^{122/118}$Sn of 0.37 ± 0.04 ‰ and 0.35 ± 0.06 ‰, respectively). Moreover, the BCR-2 and BHVO-2 full replicates were used to test the effect of HF addition in the collecting beaker and before each sample evaporation on the final yield. Both these HF additions significantly increase the yield by factors of 4 and 6 respectively, and the combination of both could increase the yields from 2 to 7 times (see Table S-2). Overall, this demonstrates the robustness of the double-spike method in correcting for possible fractionations associated to significant Sn loss occurring during the chemical processing and purification protocols necessary for Sn isotopic measurements.

Supplementary Tables

Table S-1 Tin isotopic compositions of twenty-four glacial diamictites and two geological reference materials.

Stratigraphic unit	Location	Depositional age (Ga)	Reference	Sn (ppm)	$\delta^{122/118}Sn_{NIST3161a}$ (‰)	2 s.d.	*n*
Archean							
Afrikander	South Africa	2.96	Guy *et al.* (2010)	0.39	0.19	0.01	1
Coronation	South Africa	2.96	Guy *et al.* (2010)	1.58	0.20	0.01	1
Mozaan	South Africa	2.97	Young *et al.* (1998)	0.95	0.38	0.01	1
Promise	South Africa	2.96	Guy *et al.* (2010)	0.89	0.20	0.01	1
Palaeoproterozoic							
Bottle Creek	USA	2.28	Houston *et al.* (1992)	1.05	0.26	0.04	3
Bruce	Canada	2.38	Melezhik *et al.* (2013)	1.72	0.00	0.02	3
Duitschland	South Africa	2.38	Melezhik *et al.* (2013)	3.56	0.19	0.01	1
Gowganda	Canada	2.40	Melezhik *et al.* (2013)	1.33	0.15	0.03	2
Makganyene	South Africa	2.44	Melezhik *et al.* (2013)	2.08	0.15	0.01	2
Ramsay Lake	Canada	2.44	Melezhik *et al.* (2013)	1.36	0.28	0.01	1
Timeball Hill	South Africa	2.25	Melezhik *et al.* (2013)	2.67	0.17	0.00	2
Neoproterozoic							
Blaubeker	Namibia	0.69	Prave *et al.* (2011)	1.89	0.25	0.01	3
Chuos	Namibia	0.69	Le Heron *et al.* (2013)	1.60	0.22	0.01	4
Gaskiers	Canada	0.58	Carto and Eyles (2011)	1.87	0.24	0.00	2
Ghaub	Namibia	0.64	Hoffman (2011)	1.54	0.21	0.01	3
Gucheng	China	0.68	Liu *et al.* (2008)	2.24	0.25	0.01	1
Kaigas	Namibia	0.76	Frimmel (2011)	3.93	0.24	0.01	3
Konnarock	USA	0.67	Rankin (1993)	2.63	0.32	0.02	2
Nantuo	China	0.65	Zhou *et al.* (2004)	2.49	0.21	0.01	1
Numees	Namibia	0.65	Frimmel (2011)	2.38	0.24	0.01	3
Pocatello	USA	0.69	Keeley *et al.* (2013)	3.03	0.23	0.02	2
Palaeozoic							
Bolivia	South America	0.32	Starck and del Papa (2006)	2.68	0.23	0.01	1
Dwyka East	South Africa	0.30	Visser (1982)	2.31	0.26	0.03	3
Dwyka West	South Africa	0.30	Visser (1982)	1.38	0.21	0.01	1
Reference materials							
BHVO-2					0.36	0.03	7
BCR-2					0.28	0.03	11

Table S-2 Results testing the chemical protocol on six full replicates of reference materials. The addition of concentrated HF in the beaker before evaporation and in the collecting beaker is tested as a potential factor influencing the separation yield and isotopic ratios. Although the yield is positively affected by these additional steps in the protocol, the measured isotopic compositions are identical within error.

Sample	Conc. HF in beaker before evaporation	Conc. HF in collecting beaker	*n*	Yield (%)	$\delta^{122/118}$Sn	2 s.d.
BHVO-2			4	20.7	0.37	0.04
BHVO-2	X	X	3	40.3	0.35	0.06
BCR-2			2	7.6	0.29	0.01
BCR-2	X		3	45.6	0.29	0.03
BCR-2		X	3	29.5	0.27	0.04
BCR-2	X	X	3	48.4	0.27	0.02

Supplementary Information References

Carto, S.L., Eyles, N. (2011) The deep-marine glaciogenic Gaskiers Formation, Newfoundland, Canada. In: Arnaud, E., Halverson, G.P., Shields-Zhou, G. (Eds.) *The Geological Record of Neoproterozoic Glaciations*. Geological Society Memoir 36, Geological Society, London, 467–473. https://doi.org/10.1144/M36.42

Creech, J.B., Paul, B. (2015) IsoSpike: Improved Double-Spike Inversion Software. *Geostandards and Geoanalytical Research* 39, 7–15. https://doi.org/10.1111/j.1751-908X.2014.00276.x

Creech, J.B., Moynier, F., Badullovich, N. (2017) Tin stable isotope analysis of geological materials by double-spike MC-ICPMS. *Chemical Geology* 457, 61–67. https://doi.org/10.1016/j.chemgeo.2017.03.013

Frimmel, H.E. (2011) The Kaigas and Numees formations, Port Nolloth Group, in South Africa and Namibia. In: Arnaud, E., Halverson, G.P., Shields-Zhou, G. (Eds.) *The Geological Record of Neoproterozoic Glaciations*. Geological Society Memoir 36, Geological Society, London, 223–231. https://doi.org/10.1144/M36.17

Gaschnig, R.M., Rudnick, R.L., McDonough, W.F., Kaufman, A.J., Valley, J.W., Hu, Z., Gao, S., Beck, M.L. (2016) Compositional evolution of the upper continental crust through time, as constrained by ancient glacial diamictites. *Geochimica et Cosmochimica Acta* 186, 316–343. https://doi.org/10.1016/j.gca.2016.03.020

Guy, B.M., Beukes, N.J., Gutzmer, J. (2010) Paleoenvironmental controls on the texture and chemical composition of pyrite from non-conglomeratic sedimentary rocks of the Mesoarchean Witwatersrand Supergroup, South Africa. *South African Journal of Geology* 113, 195–228. https://doi.org/10.2113/gssajg.113.2.195

Hoffman, P.F. (2011) Strange bedfellows: glacial diamictite and cap carbonate from the Marinoan (635 Ma) glaciation in Namibia. *Sedimentology* 58, 57–119. https://doi.org/10.1111/j.1365-3091.2010.01206.x

Houston, R.S., Karlstrom, K.E., Graff, P.J., Flurkey, A.J. (1992) *New stratigraphic subdivisions and redefinition of subdivisions of late Archean and early Proterozoic metasedimentary and metavolcanic rocks of the Sierra Madre and Medicine Bow Mountains, southern Wyoming*. USGS Professional Paper 1520, U.S. Geological Survey, Washington, D.C. https://doi.org/10.3133/pp1520

Keeley, J.A., Link, P.K., Fanning, C.M., Schmitz, M.D. (2013) Pre- to synglacial rift-related volcanism in the Neoproterozoic (Cryogenian) Pocatello Formation, SE Idaho: New SHRIMP and CA-ID-TIMS constraints. *Lithosphere* 5, 128–150. https://doi.org/10.1130/L226.1

Le Heron, D.P., Busfield, M.E., Kamona, F. (2013) An interglacial on snowball Earth? Dynamic ice behaviour revealed in the Chuos Formation, Namibia. *Sedimentology* 60, 411–427. https://doi.org/10.1111/j.1365-3091.2012.01346.x

Liu, X., Gao, S., Diwu, C., Ling, W. (2008) Precambrian crustal growth of Yangtze Craton as revealed by detrital zircon studies. *American Journal of Science* 308, 421–468. https://doi.org/10.2475/04.2008.02

Melezhik, V.A., Young, G.M., Eriksson, P.G., Altermann, W., Kump, L.R., Lepland, A. (2013) 7.2 Huronian-Age Glaciation. In: Melezhik, V.A., Prave, A.R., Hanski, E.J., Fallick, A.E., Lepland, A., Kump, L.R., Strauss, H. (Eds.) *Reading the Archive of Earth's Oxygenation, Volume 3: Global Events and the Fennoscandian Arctic Russia-Drilling Early Earth Project*. Springer, Berlin, Heidelberg, 1059–1109. https://doi.org/10.1007/978-3-642-29670-3_2

Prave, A.R., Hoffmann, K.-H., Hegenberger, W., Fallick, A.E. (2011) The Witvlei Group of East-Central Namibia. In: Arnaud, E., Halverson, G.P., Shields-Zhou, G. (Eds.) *The Geological Record of Neoproterozoic Glaciations*. Geological Society Memoir 36, Geological Society, London, 211–216. https://doi.org/10.1144/M36.15

Rankin, D.W. (1993) The volcanogenic Mount Rogers Formation and the overlying glaciogenic Konnarock Formation: Two late Proterozoic units in southwestern Virginia. USGS Bulletin 2029, U.S. Geological Survey, Washington, D.C. https://doi.org/10.3133/b2029

She, J.-X., Kubik, E., Li, W., Moynier, F. (2023) Stable Sn isotope signatures of Mid-ocean ridge basalts. *Chemical Geology* 622, 121347. https://doi.org/10.1016/j.chemgeo.2023.121347

Starck, D., del Papa, C. (2006) The northwestern Argentina Tarija Basin: Stratigraphy, depositional systems, and controlling factors in a glaciated basin. *Journal of South American Earth Sciences* 22, 169–184. https://doi.org/10.1016/j.jsames.2006.09.013

Visser, J.N.J. (1982) Upper Carboniferous glacial sedimentation in the Karoo Basin near Prieska, South Africa. *Palaeogeography, Palaeoclimatology, Palaeoecology* 38, 63–92. https://doi.org/10.1016/0031-0182(82)90065-7

Young, G.M., Von Brunn, V., Gold, D.J.C., Minter, W.E.L. (1998) Earth's Oldest Reported Glaciation: Physical and Chemical Evidence From the Archean Mozaan Group (~2.9 Ga) of South Africa. *The Journal of Geology* 106, 523–538. https://doi.org/10.1086/516039

Zhou, C., Tucker, R., Xiao, S., Peng, Z., Yuan, X., Chen, Z. (2004) New constraints on the ages of Neoproterozoic glaciations in south China. *Geology* 32, 437–440. https://doi.org/10.1130/G20286.1